

# Lawrence Berkeley National Laboratory

## LBL Publications

### Title

Cyclic Fatigue-Crack Propagation in a Silicon-Carbide Whisker Reinforced Alumina Composite: Role of Load Ratio

### Permalink

<https://escholarship.org/uc/item/5xz7k6mw>

### Authors

Dauskardt, R.H.  
Dagleish, B.J.  
Yao, D.  
et al.

### Publication Date

1992-03-01



# Lawrence Berkeley Laboratory

UNIVERSITY OF CALIFORNIA

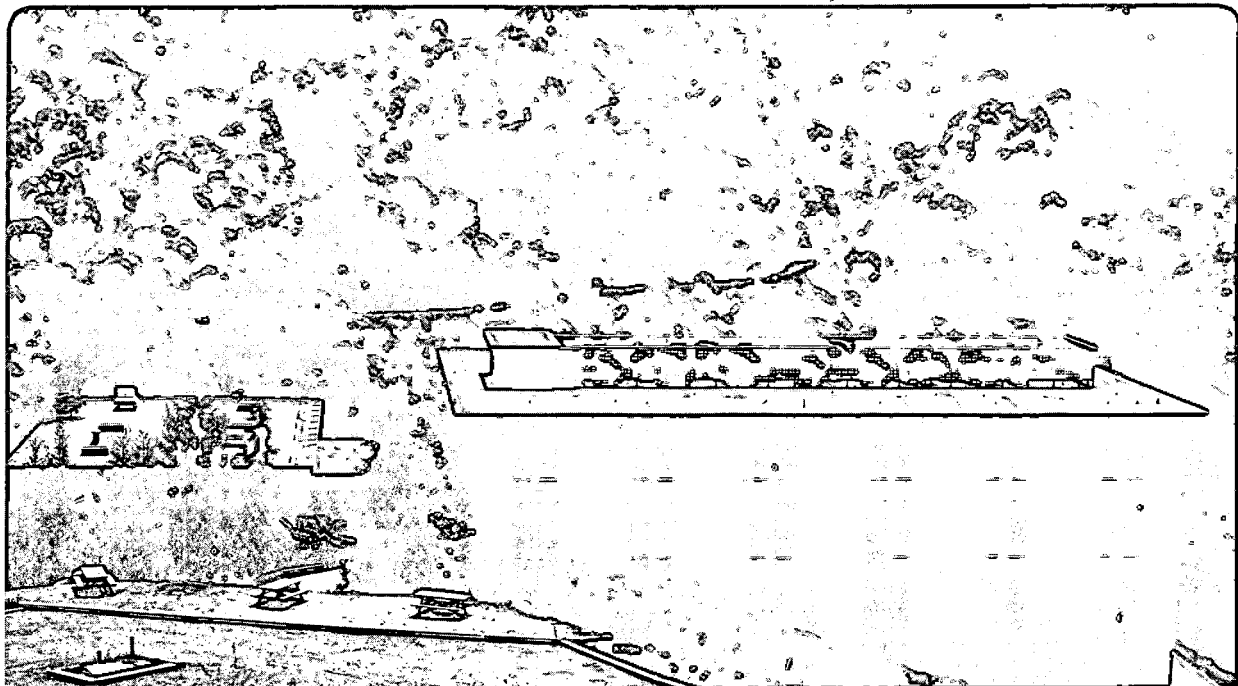
## Materials Sciences Division

Submitted to Journal of Materials Science

### Cyclic Fatigue-Crack Propagation in a Silicon-Carbide Whisker Reinforced Alumina Composite: Role of Load Ratio

R.H. Dauskardt, B.J. Dalgleish, D. Yao, P.F. Becher, and R.O. Ritchie

March 1992



LOAN COPY  
Circulates  
for 4 weeks

Bldg. 50 Library.

LBL-32807

Copy 2

## **DISCLAIMER**

This document was prepared as an account of work sponsored by the United States Government. While this document is believed to contain correct information, neither the United States Government nor any agency thereof, nor the Regents of the University of California, nor any of their employees, makes any warranty, express or implied, or assumes any legal responsibility for the accuracy, completeness, or usefulness of any information, apparatus, product, or process disclosed, or represents that its use would not infringe privately owned rights. Reference herein to any specific commercial product, process, or service by its trade name, trademark, manufacturer, or otherwise, does not necessarily constitute or imply its endorsement, recommendation, or favoring by the United States Government or any agency thereof, or the Regents of the University of California. The views and opinions of authors expressed herein do not necessarily state or reflect those of the United States Government or any agency thereof or the Regents of the University of California.

**CYCLIC FATIGUE-CRACK PROPAGATION IN A SILICON-CARBIDE WHISKER  
REINFORCED ALUMINA COMPOSITE: ROLE OF LOAD RATIO**

**Reinhold H. Dauskardt,<sup>1</sup> Brian J. Dalgleish,<sup>1</sup> Daping Yao,<sup>1</sup>  
Paul F. Becher<sup>2</sup> and Robert O. Ritchie<sup>1</sup>**

<sup>1</sup>Center for Advanced Materials, Materials Sciences Division  
Lawrence Berkeley Laboratory  
and  
Department of Materials Science and Mineral Engineering  
University of California, Berkeley, CA 94720

and

<sup>2</sup>Metals and Ceramics Division  
Oak Ridge National Laboratory, Oak Ridge, TN 37831

March 1992

submitted to  
*Journal of Materials Science*

# CYCLIC FATIGUE-CRACK PROPAGATION IN A SILICON-CARBIDE WHISKER REINFORCED ALUMINA COMPOSITE: ROLE OF LOAD RATIO

Reinhold H. Dauskardt,<sup>1</sup> Brian J. Dalgleish,<sup>1</sup> Daping Yao,<sup>1\*</sup>  
Paul F. Becher<sup>2</sup> and Robert O. Ritchie<sup>1</sup>

<sup>1</sup>Center for Advanced Materials, Materials Sciences Division,  
Lawrence Berkeley Laboratory  
and Department of Materials Science and Mineral Engineering,  
University of California, Berkeley, CA 94720

<sup>2</sup>Metals and Ceramics Division, Oak Ridge National Laboratory, Oak Ridge, TN 37831

## ABSTRACT

The characteristics of subcritical crack growth by cyclic fatigue have been examined in a silicon-carbon whisker reinforced alumina composite, with specific reference to the role of load ratio (ratio of minimum to maximum applied stress intensity,  $R = K_{\min}/K_{\max}$ ); results are compared with similar subcritical crack-growth data obtained under constant load conditions (static fatigue). Using compact-tension samples cycled at ambient temperatures, cyclic fatigue-crack growth has been measured over six orders of magnitude from  $\sim 10^{-11}$  to  $10^{-5}$  m/cycle at load ratios ranging from 0.05 to 0.5. Growth rates ( $da/dN$ ) display an approximate Paris power-law dependence on the applied stress-intensity range ( $\Delta K$ ), with an exponent varying between 33 and 50. Growth-rate behavior is found to be strongly dependent upon load ratio; the fatigue threshold  $\Delta K_{TH}$ , for example, is found to be increased by over 80% at  $R = 0.05$  compared to  $R = 0.5$ . These results are rationalized in terms of a far greater dependency of growth rates on  $K_{\max}$  ( $da/dN \propto K_{\max}^{30}$ ) compared to  $\Delta K$  ( $da/dN \propto \Delta K^5$ ), in contrast to fatigue behavior in metallic materials where generally the reverse is true. Micromechanisms of crack advance underlying such behavior are discussed in terms of time-dependent crack bridging involving either matrix grains or unbroken whiskers.

## 1. Introduction

Until recently, it had been the general perception that ceramic materials are largely insensitive to mechanical degradation under cyclic loads [1]. However, several studies, primarily over the past five years, have provided conclusive evidence that indeed ceramics do suffer cyclic fatigue under both tensile and compressive loading [see refs. 2-4 for review]. Results for both monolithic and composite ceramics have shown reduced lifetimes during stress/life (S/N) testing under cyclic, compared to quasi-static, loads, and accelerated cyclic crack-propagation rates at stress intensities less than that required for environmentally-enhanced crack growth (static fatigue) during fracture-mechanics testing.

---

\*Presently in the Department of Materials Science and Engineering, University of Illinois - Urbana-Champaign, Urbana, IL 61801.

Compared to metals, cyclic fatigue-crack propagation data for a wide range of ceramic materials display a marked power-law dependency of growth rates on the applied (far-field) stress-intensity range ( $\Delta K = K_{\max} - K_{\min}$ ). In simple terms, the crack-growth increment per cycle,  $da/dN$ , can be related to the applied  $\Delta K$  (for "long" cracks typically in excess of a few mm in length) via a Paris power-law expression of the form [5]:

$$da/dN = C (\Delta K)^m, \quad (1)$$

where  $C$  and the exponent  $m$  are experimentally measured scaling constants dependent on the material and environmental conditions. Essentially, this behavior is qualitatively similar to metallic materials (between typically  $\sim 10^{-9}$  and  $\sim 10^{-6}$  m/cycle); however, unlike metals, the exponent  $m$  can take values as high as 50 and above in ceramics [2], compared to typical values of between 2 and 4 in metals.

The very high exponents in Eq. 1 reported for ceramics result from a particularly marked sensitivity of growth rates to the maximum stress-intensity factor,  $K_{\max}$  of the loading cycle (and likewise the load ratio  $R = K_{\min}/K_{\max}$ ) [6-7]. As recently shown for SiC-reinforced alumina [7], by explicitly including  $K_{\max}$  in the growth-rate relationship, viz.\*

$$da/dN = C' (K_{\max})^n (\Delta K)^p, \quad (2)$$

---

\*This is equivalent to the empirical model of Walker [8] commonly used to normalize load-ratio effects in metal fatigue, where an effective stress intensity,  $K_{\text{eff}}$ , is defined such that  $K_{\text{eff}} = K_{\max} (1 - R)^{\alpha}$ , where  $\alpha$  is a material property equal to  $p/(p + n)$ .

---

where  $C'$  is a constant equal to  $C(1 - R)^n$  and  $(n + p) = m$ , the power-law dependencies of the growth rates on  $K_{\max}$  and  $\Delta K$ , as indicated by the exponents  $n$  and  $p$ , were found to be 10.2 and 4.8, respectively; this is to be compared with values of  $n = 0.4$  and  $p = 3$  for metal fatigue of a nickel-base superalloy [9]. The marked sensitivity of growth rates to  $K_{\max}$  (or the load ratio) is similar to that seen in metals at high growth rates approaching instability, e.g., where  $K_{\max}$  approaches the fracture toughness,  $K_{Ic}$ ; under these conditions, mechanisms

of crack growth predominantly involve static fracture modes (e.g., cleavage, microvoid coalescence, etc.) akin to mechanisms that occur under (quasi-static) monotonic loading [10]. Moreover, it is consistent with subcritical crack-growth data for both fine-grained monolithic and toughened (PSZ, whisker-reinforced alumina) ceramics under constant loading (static fatigue, stress-corrosion cracking), where crack velocities are given in terms of the applied stress intensity  $K$  by [11-13]:

$$da/dt = v = A K^s . \quad (3)$$

Similar to the exponent "n" in the cyclic-fatigue relationship in Eq. 2, values of "s" are very high with values up to  $\sim 100$  [11-13].

The intent of the present study is to investigate the separate effects of  $K_{max}$  and  $\Delta K$  on cyclic fatigue-crack growth behavior in an alumina ceramic reinforced with strong, microscopic SiC whiskers. Cyclic crack-growth rates are measured over a range of load ratios and are compared with corresponding static-fatigue data obtained under constant load. Implications of the observed crack-growth dependence on both  $K_{max}$  and  $\Delta K$  are discussed in light of possible micro-mechanisms for crack advance and crack-tip shielding.

## 2. Experimental procedures

### 2.1. Material

Experiments were conducted on nominally fully dense samples of a SiC-whisker reinforced aluminas ( $Al_2O_3$ -SiC<sub>w</sub>), as shown in Fig. 1; whisker volume fractions of 20 and 28% were examined. The composites were prepared at Oak Ridge National Laboratory by hot pressing granulated powder consisting of a mixture of high purity alumina powder and SiC whiskers in an inert environment. No other additives were incorporated during processing. The resulting microstructure consisted of  $< 2$ - $\mu$ m-sized alumina grains containing a uniform dispersion of  $\sim 0.8$ - $\mu$ m-diameter SiC whiskers; the whiskers had an as-received aspect ratio of up to 40, were predominantly of the  $\alpha$  (hexagonal) form, and tended to be oriented perpendicularly to

the hot-pressing direction. Some degree of local porosity was evident in the microstructure, particularly at clusters of whiskers (Fig. 1b). Further details of the processing techniques and microstructure are reported elsewhere [14,15].

Tests specimens for both cyclic and static fatigue tests were prepared from a hot pressed composite with the specimen oriented so that the crack plane was parallel to the axis of the hot press die. The orientations of the long axis of the whiskers tended to lie near normal to the axis of hot pressing but were randomly oriented within the plane normal to the axis of hot pressing. Therefore, the specimen orientation used provided maximum interaction between the crack and the SiC whiskers. Two different composite compositions were tested; some of the characteristics of each are shown in Table I, and are compared with those of monolithic alumina.

**Table I. Characteristics of SiC Whisker<sup>a</sup> Reinforced Alumina Composites**

| Sample Number       | Whisker Content Vol % | Density g/cc | % of Theoretical Density | Alumina Grain Size $\mu\text{m}$ | Fracture Toughness $\text{MPa}\sqrt{\text{m}}$ | Fracture Strength MPa |
|---------------------|-----------------------|--------------|--------------------------|----------------------------------|--|-----------------------|
| WRA-10 <sup>b</sup> | 28                    | 3.73         | 99.0                     | 1.5                              | $8.7 \pm 0.9$                                  | —                     |
| SC-83 <sup>c</sup>  | 20                    | 3.82         | 99.9                     | 9                                | $8.7 \pm 1.1$                                  | $587 \pm 27$          |
| Al-CR10-13          | 0                     | 3.96         | 99.5                     | 4                                | $4.6 \pm 0.5$                                  | 250                   |

<sup>a</sup> SiC whiskers F-9, Advanced Composite Materials Corp., Greer, SC.

<sup>b</sup> Alumina powder (CR-10), Baikowski Corp., Charlotte, NC.

<sup>c</sup> Alumina powder (Linde A), Union Carbide Corp., Indianapolis, IN.

## 2.2. Test Methods

**2.2.1. Cyclic Fatigue:** Cyclic crack-growth rates were determined under computer-controlled K-decreasing and K-increasing conditions using 3-mm thick compact-tension C(T) specimens containing long ( $> 3$  mm) through-thickness cracks (Fig. 2). Tests were performed using high-resolution, computer-controlled electro-servo-hydraulic testing machines in general accordance with the ASTM Standard for measurement of fatigue-crack growth rates in metals



[16], modified for ceramics using the procedures outlined by Dauskardt and Ritchie [17]. Specimens were cycled at a frequency of 25 Hz (sine wave) at selected load ratios (ratio of minimum to maximum applied loads) of 0.05, 0.1, 0.3 and 0.5; the test environment was controlled room air at  $22 \pm 2^\circ\text{C}$  with  $45 \pm 5\%$  relative humidity. Growth rates were measured over the range  $\sim 10^{-5}$  to  $10^{-11}$  m/cycle to approach a fatigue threshold, below which crack growth could not be experimentally detected. In the present experiments, thresholds are operationally defined in terms of the maximum and alternating stress intensity ( $K_{\text{max,TH}}$ ,  $\Delta K_{\text{TH}}$ ) at which growth rates do not exceed  $10^{-11}$  m/cycle. Further experimental details are given elsewhere [17].

Crack lengths were monitored *in situ* to a resolution better than  $\pm 2 \mu\text{m}$ , using electrical-potential measurements across  $\sim 0.1\text{-}\mu\text{m}$ -thick NiCr foils evaporated onto the specimen surface [17,18]. Such measurements were confirmed by periodically measuring the crack length using optical techniques. Back-face strain compliance measurements, from strain gauges bonded onto the back face of the specimen, were used to estimate the extent of fatigue crack closure [19]; the closure phenomenon results from premature contact of the crack faces on unloading due to the wedging action of, for example, fracture-surface asperities behind the crack tip [20,21]. The degree of crack closure was assessed in terms of the closure stress intensity,  $K_{\text{cl}}$ , defined at first contact of the crack surfaces during the unloading cycle; specifically, the value of  $K_{\text{cl}}$  was calculated from the highest load where the elastic unloading line deviated from linearity (Fig. 2) [19]. Such measurements provide a global measure of the closure stress intensity; however, they are typically insensitive to changes in closure in the immediate vicinity of the crack tip [22,23], and, as discussed below, are difficult to interpret in material systems such as  $\text{Al}_2\text{O}_3\text{-SiC}$  where additional crack-surface contact may occur due to non-wedging phenomena such as crack bridging [24].

**2.2.2. Static Fatigue:** Crack-growth rates under constant-loading conditions were determined using precracked ( $\geq 4$  mm long precrack) applied-moment double cantilever-beam (AMDCB) specimens. For this specimen geometry, the applied stress intensity is independent of the crack length; thus for a given specimen size, the stress intensity can be varied simply by changing the load. In the current tests, the AMDCB samples were dead-weight loaded to raise and lower the stress intensity, and the crack-tip position was periodically monitored using an optical cathometer system which could resolve the crack tip to within  $\pm 2 \mu\text{m}$  on the mechanically polished side surface of the test sample. The temperature and relative humidity were maintained at  $22 \pm 2^\circ\text{C}$  and  $55 \pm 5\%$ , respectively.

**2.2.3. Fracture Toughness:** Fracture toughness,  $K_{Ic}$ , values were obtained using the multiple indent flexure strength test method [25]. Highly polished four-point flexure bars were used with roughly five Vicker's hardness indents located on the tensile surface to provide the stress concentrator.  $K_{Ic}$  values were then estimated in the usual manner from the (maximum) load and crack length immediately prior to failure. The indentation load used was 98.07 N (10 kg).

**2.2.4. Fractography:** Fracture surfaces were examined using optical and scanning electron microscopy, and in profile using planar sections cut perpendicular to the crack path in the plane of loading.

### **3. Results and discussion**

#### **3.1. Static Fatigue-Growth Rate Behavior**

The results for the crack growth studies are shown in Fig. 3 for aluminas reinforced with 20 and 28 vol. % SiC whiskers and are compared to those for a dense (99.9% of theoretical density) alumina ceramic with an average grain size of  $4 \mu\text{m}$  (or about one half that of the composite with 20 vol. % SiC whiskers). It is clear that the onset of slow crack growth under constant loading requires a much higher applied stress intensity in the reinforced aluminas

(which show essentially identical  $v/K$  behavior). In fact, the applied stress intensity required to achieve a crack velocity of  $\sim 10^{-10}$  m/s in the composites is twice that required for the unreinforced alumina. Analysis of the crack-growth response can be made based on the power-law relationship in Eq. 3; values of the constant A and exponent "s" are listed in Table II. Regression analysis of the data represented in this form indicates a very strong dependence of the crack velocity upon the applied stress intensity for both materials, as indicated by the high "s" values in Table II.

**Table II. Static Fatigue-Crack Growth Parameters for  $Al_2O_3$  and  $Al_2O_3$ -SiC<sub>w</sub> Composites**

| Sample   | A<br>(m/s (MPa $\sqrt{m}$ ) <sup>-s</sup> ) | s  | K <sub>TH</sub><br>(MPa $\sqrt{m}$ ) |
|--|---|----|--------------------------------------|
| $Al_2O_3$<br>( $\sim 4 \mu\text{m}$ grain size)                            | $1.3 \times 10^{-38}$                       | 55 | 3.2                                  |
| $Al_2O_3$ -20 vol.% SiC <sub>w</sub><br>( $\sim 9 \mu\text{m}$ grain size) | $2.7 \times 10^{-80}$                       | 81 | 7.1                                  |
| $Al_2O_3$ -28 vol.% SiC <sub>w</sub>                                       | $7.2 \times 10^{-75}$                       | 75 | 7.0                                  |

### 3.2. Cyclic Fatigue-Growth Rate Behavior

Corresponding cyclic fatigue-crack growth rate data for load ratios of 0.05, 0.1, 0.3 and 0.5 are plotted in Fig. 4 as a function of the applied  $\Delta K$ . The  $Al_2O_3$ -28 vol.% SiC<sub>w</sub> composite displays extensive cyclic fatigue-crack propagation over six orders of magnitude in growth rates; in fact, similar to metals [26], the growth-rate curves show a slightly sigmoidal shape which was reproducible under both increasing and decreasing stress-intensity conditions. Furthermore, as in metal fatigue [26], growth rates are increased, and fatigue threshold  $\Delta K_{TH}$  values decreased, with increasing R; for example,  $\Delta K_{TH}$  values are increased by over 80% at  $R = 0.05$  compared to  $R = 0.5$ . If these data are fitted to a conventional Paris law relationship (of the form of Eq. 1), similar to the static-fatigue data, growth rates can be seen to display a marked power-law dependence on the applied stress intensity ranging from 33 to

50; moreover, values of the threshold  $K_{\max,TH}$  were found to be approximately 65% of  $K_{Ic}$ . Both observations are similar to behavior reported for other ceramic materials [2,3]. Values of  $C$ ,  $m$  and  $\Delta K_{TH}$  at the selected load ratios are listed in Table III.

To examine the specific dependence to  $K_{\max}$  and  $\Delta K$ , growth-rate data were also fitted to Eq. 2. In these terms, it is apparent that the steep Paris law exponents,  $m$ , are associated with a marked sensitivity of growth rates to  $K_{\max}$  rather than  $\Delta K$ ; corresponding values of  $n$  and  $p$  are  $\sim 30$  and  $5$ , respectively. Resistance to cyclic fatigue-crack growth, as indicated by the value of  $\Delta K_{TH}$ , is clearly sensitive to the load ratio and the entire growth-rate curve is shifted to lower values on the abscissa with increasing values of  $R$ . While such behavior is similar to near-threshold growth rates in metallic materials where  $\Delta K_{TH}$  levels are invariably decreased at higher load ratios [e.g., ref. 26], behavior at higher (intermediate) growth rates (i.e.,  $\sim 10^{-9}$  to  $10^{-6}$  m/cycle) is generally far less sensitive to the load ratio.\* In fact, the effect of load ratio on growth-rate behavior can be effectively normalized by plotting the  $da/dN$  data

---

\*Note that at very high growth rates ( $\geq 10^{-6}$  m/cycle) approaching instability, e.g., as  $K_{\max}$  approaches  $K_{Ic}$ , the marked dependence of growth rates on mean stress (or load ratio) often reappears in metallic materials as the mechanism of fatigue-crack growth involves the occurrence of "static" fracture modes, i.e., microvoid coalescence, cleavage, intergranular cracking, all mechanisms which are strongly sensitive to the tensile or hydrostatic stresses, rather than the alternating stresses per se [10].

---

as a function of the maximum stress intensity,  $K_{\max}$  (Fig. 5); the fatigue threshold, expressed in terms of a maximum stress intensity,  $K_{\max,TH}$ , is essentially constant and independent of  $R$ . By representing the current results in this way, it is apparent that at a given stress intensity the velocity (with respect to time) of cyclic fatigue cracks in the  $Al_2O_3-SiC_w$  composite far exceeds that of static fatigue cracks in this material [11,27], thereby re-affirming the essential role of the unloading cycle for the cyclic-fatigue process to occur. Crack velocities, however, are significantly slower than corresponding static fatigue-crack growth in the unreinforced  $Al_2O_3$  matrix.

**Table III. Cyclic Fatigue-Crack Growth Parameters for Al<sub>2</sub>O<sub>3</sub>-28 vol.% SiC<sub>w</sub> Composite**

| Load Ratio<br>R | C<br>(m/cycle (MPa√m) <sup>-m</sup> ) | m  | ΔK <sub>TH</sub><br>(MPa√m) | K <sub>max,TH</sub><br>(MPa√m) |
|-----------------|---------------------------------------|----|-----------------------------|--------------------------------|
| 0.05            | 5.9 × 10 <sup>-34</sup>               | 33 | 5.3                         | 5.5                            |
| 0.10            | 1.6 × 10 <sup>-44</sup>               | 48 | 5.2                         | 5.7                            |
| 0.30            | 3.5 × 10 <sup>-33</sup>               | 37 | 4.1                         | 5.9                            |
| 0.50            | 7.3 × 10 <sup>-34</sup>               | 50 | 2.9                         | 5.9                            |

### 3.3. Fatigue Crack Closure

Similar to behavior widely reported for metals [e.g., refs. 20,21] and in limited cases for ceramics [2,7,23], cyclic fatigue-crack growth behavior in the Al<sub>2</sub>O<sub>3</sub>-28 vol.% SiC<sub>w</sub> composite showed evidence of crack-surface contact (i.e., "crack closure") during the fatigue loading cycle. Far-field crack-closure levels, defined in terms of K<sub>cl</sub> and corresponding to the growth-rate data in Fig. 4 for each load ratio, are given in Fig. 6. Such closure in Al<sub>2</sub>O<sub>3</sub>-SiC<sub>w</sub> appears to be caused by premature contact of rough asperities on the crack surfaces during the unloading cycle prior to minimum load. The resulting wedging effect acts to raise the effective minimum stress intensity (K<sub>min</sub> ≡ K<sub>cl</sub>), thereby lowering the effective range of stress intensity ΔK<sub>eff</sub> (K<sub>max</sub> - K<sub>cl</sub>, for K<sub>cl</sub> > K<sub>min</sub>) actually experienced by the crack tip [20]. In metallic materials, replotting the growth rates for various positive load ratios in terms of ΔK<sub>eff</sub>, rather than ΔK, generally will normalize the growth-rate data, as the effect of load ratio on crack velocities, particularly at near-threshold levels, is primarily associated with crack closure; higher R ratios minimize the wedging effect of closure as they involve larger crack opening displacements [19-21]. However with ceramics, this approach can be seen in Fig. 7 to have only limited success. Compared to behavior in metallic materials [e.g., ref. 21], the role of crack closure in influencing cyclic crack growth in ceramic materials remains poorly understood. There is little doubt that the crack wedging action of, for example, fracture-surface asperities will tend to diminish the crack-driving force, and as such act to retard

crack-extension rates as in metals. However, whether such phenomena can be quantified in terms of a closure stress intensity remains uncertain, given that the experimental measurement of  $K_{cl}$  in terms of crack-surface contact may be clouded in many ceramics by the occurrence of other shielding mechanisms [28] such as whisker or matrix-grain bridging.

### 3.4. *Fractography*

Scanning electron microscopy observations of the static-fatigue fracture surfaces produced at crack velocities of  $\sim 10^{-3}$  m/s reveal substantial amount of transgranular fracture through the alumina grains and evidence of SiC whisker bridging and pullout (Fig. 8). Whisker pullout is supported by the whiskers extending above the fracture surface and by the holes where the ends of whiskers have been extracted from the matrix during fracture.

Corresponding micrographs of the fracture surfaces during overload fracture and fatigue-crack propagation at  $R = 0.05, 0.3$  and  $0.5$  are shown in Fig. 9. Fracture surfaces are again characterized by two primary features, namely transgranular cleavage of the matrix grains (*marked by the letter A in Fig. 9*) interdispersed with the fracture and pull-out of the SiC whiskers (*marked B*). The fracture morphology is only marginally changed at the differing load ratios and is in fact very similar for failure under either monotonic or cyclic loading. However, there is evidence of somewhat more whisker pull-out in cyclic fatigue and more matrix-grain cleavage under monotonic loads (c.f., Fig. 9d & 9a). Moreover, for the cyclic fatigue surfaces, the proportion of transgranular cleavage facets does appear to increase slightly with increasing load ratio.

On examination of the cyclic fatigue fractures by metallographic sectioning (Fig. 10), it is apparent that that the crack path frequently tends to seek out regions of local porosity (*marked by the letter C in Fig. 10*). The interaction of the fatigue crack with the SiC whiskers in general involves either whisker fracture (*marked D*) or debonding along the whisker/matrix interface (*marked E*), with little change in crack-path direction; however, there are examples of significant crack deflection where the crack encounters the larger whiskers (*marked F*). *In*

*situ* observations of crack propagation reveal the occurrence of matrix-grain bridging behind the crack tip; however, no evidence of crack bridging by intact whiskers could be detected.

### 3.5. *Mechanisms of Crack Growth*

Previous studies [14,15,28,29] on monotonic crack propagation and fracture-toughness behavior have shown that the principal contributions to crack-growth resistance in the present  $\text{Al}_2\text{O}_3$ - $\text{SiC}_w$  composite system result from crack bridging by partially bonded SiC whiskers, subsequent pullout of these whiskers, bridging and pullout of matrix grains, and to a small extent from crack deflection. The increases in toughness induced by the bridging processes derive from tractions imposed on the crack surfaces by the whiskers and grains, which vary with increases in the crack opening displacement behind the crack tip.

For frictional bridging by partially debonded whiskers, large radial stresses are imposed on the debonding interfaces by the thermal expansion mismatch between SiC and  $\text{Al}_2\text{O}_3$ . Thus, although the whiskers are relatively strong (~8 to 16 GPa) [30], the bridging stresses supported by these whiskers increase very rapidly as the crack opens such that whisker fracture ensues a short distance behind the crack tip. This implies that the zone of unbroken whiskers in the wake of the crack tip (the frictional whisker-bridging zone) is quite small; experimental measurements [29] suggest dimensions of the order of 10  $\mu\text{m}$  behind the crack tip. However, bridging via whisker pullout, where whisker rupture occurs well away from the crack plane, can be active at distances several hundreds of micrometers behind the crack tip [31]; this process requires considerable energy as the mismatch in thermal expansion imposes significant radial compressive stresses on the sliding interface.

Compared to frictional bridging via whiskers, crack bridging by interlocking matrix grains results in much lower bridging stresses; however, the crack opening displacement required to pull out a matrix grain are much larger. Correspondingly, bridging zones for this mechanism have been estimated to extend for several hundred micrometers behind the crack tip [32,33], and are generally considered to provide a significant toughening

contribution. When the matrix grain size is very fine (e.g., less than 2  $\mu\text{m}$ ), however, matrix grain bridging appears to be far less significant for toughness than whisker bridging and pullout [15].

These multiple bridging mechanisms have been shown to combine to give an increased fracture resistance equal to the sum of the toughening contribution from each mechanism [15]. However, under cycling loading, their contribution to crack-growth resistance may be progressively diminished due to a decay of the frictional sliding resistance of the matrix/bridge interfaces. While detailed models of the micromechanics of such *time-dependent bridging* phenomena are at present not well developed, some preliminary observations [2,7,34-38] seem to suggest that wear processes during repeated sliding under the action of the cyclic loads may significantly reduce the bridging capacity of the bridging zone.

In general, such wear degradation may be expected to scale with the matrix/bridge sliding distance, resulting in a more pronounced decrease in the bridging zone capacity with *increased* cyclic crack opening displacements, that is, with decreasing load ratio, R. As discussed earlier, however, growth rates in this ceramic composite are particularly sensitive to the tensile stress state ahead of the crack tip and hence the maximum stress intensity,  $K_{\text{max}}$ , and far less sensitive to the range of stress intensity,  $\Delta K$ , as suggested by the above time-dependent bridging mechanism. Growth rates must therefore be interpreted in terms of contributions from both fracture processes *at or ahead* of the crack tip, which are particularly sensitive to  $K_{\text{max}}$  ( $da/dN \propto K_{\text{max}}^{30}$ ) and relatively insensitive to  $\Delta K$ , and wear degradation of the bridging zone capacity *behind* the crack tip, which is dependent on  $\Delta K$  ( $da/dN \propto \Delta K^5$ ). Plots of crack-growth rate data, presented in terms of  $K_{\text{max}}$ , should therefore be expected to be shifted slightly to lower stress intensities with decreasing stress-intensity range or increasing load ratio. While such behavior is only marginally apparent within the overall scatter of growth-rate data reported in the present study (Fig. 4), with improvements in the accuracy of data and more homogeneous materials, the effect is expected to be more apparent.



#### 4. Conclusions

Based on a study of the role of load ratio in influencing cyclic fatigue-crack propagation in SiC-whisker reinforced alumina-matrix composites ( $\text{Al}_2\text{O}_3\text{-SiC}_w$ ), the following conclusions can be made:

1. Rates of cyclic fatigue-crack growth ( $da/dN$ ) over the range  $\sim 10^{-11}$  to  $10^{-5}$  m/cycle are found to be power-law dependent upon the applied stress-intensity range  $\Delta K$ , with an exponent varying between 33 and 50. Similar high dependencies on the applied stress intensity are observed for static fatigue-crack growth under constant loading conditions.
2. Crack-growth rates and the value of the fatigue threshold  $\Delta K_{\text{TH}}$  are found to be strongly influenced by the load ratio (over the range  $R = 0.05$  to  $0.5$ ); specifically, values of  $\Delta K_{\text{TH}}$  are increased by over 80% at  $R = 0.05$  compared to  $R = 0.5$ . Values of  $K_{\text{max,TH}}$  are approximately 65% of  $K_{\text{Ic}}$  for all load ratios.
3. The effect of load ratio on crack-growth behavior is rationalized in terms of a far greater dependency of growth rates on the maximum, rather than the alternating, stress intensity; i.e.,  $da/dN \propto K_{\text{max}}^{30} \Delta K^5$ . Unlike metallic materials, considerations on the role of crack closure in influencing the effective crack-driving force do not provide a complete normalization of the load-ratio data.
4. The driving force for cyclic fatigue-crack growth in  $\text{Al}_2\text{O}_3\text{-SiC}_w$  is reasoned to be strongly affected by micro-mechanisms of crack bridging from interlocking matrix grains and intact whiskers and subsequent pullout. Specifically, compared to crack growth under monotonic loading, the near-tip stress intensity in cyclic fatigue is enhanced by a diminished effect of such bridging due to a time-dependent decay in the strength of the matrix/bridge interfaces.

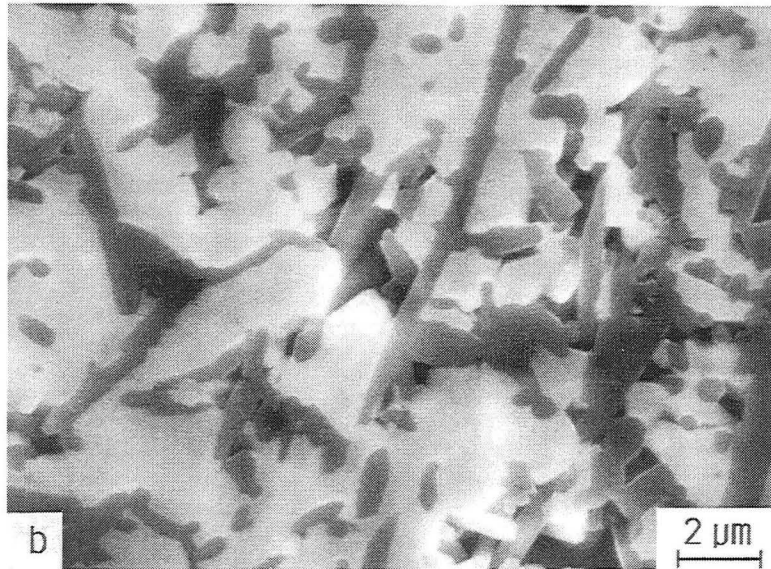
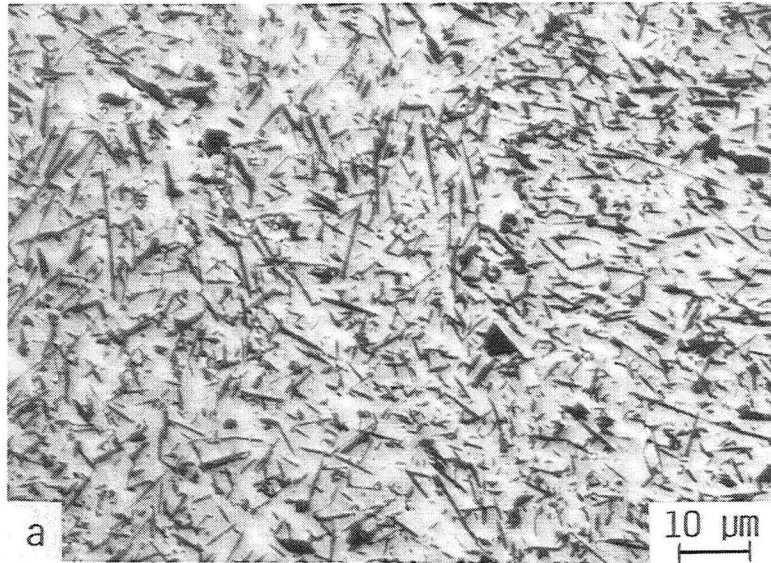
**Acknowledgments:** This work was supported by the Director, Office of Energy Research, Office of Basic Energy Sciences, Materials Sciences Division of the U.S. Department of Energy, through Contract No. DE-AC03-76SF00098 at Berkeley and Contract No. DE-AC05-84OR21400 with Martin Marietta Energy Systems, Inc. at Oak Ridge.

## References

1. A. G. EVANS, *Int. J. Fract.* **16** (1980) 485.
2. R. O. RITCHIE and R. H. DAUSKARDT, *J. Ceram. Soc. Japan* **99** (1991) 1047.
3. J. W. HOLMES, in "Flight-Vehicle Materials, Structures and Dynamics Technologies - Assessment and Future Directions," edited by A. K. Noor and F. L. Venneri, Vol. 3 (American Society for Mechanical Engineers, New York, March 1992).
4. S. SURESH, *Int. J. Fract.* **42** (1990) 41.
5. P. C. PARIS and F. ERDOGAN, *J. Bas. Eng., Trans. ASME* **85** (1963) 528.
6. S.-Y. LIU and I.-W. CHEN, *J. Am. Ceram. Soc.* **74** (1991) 1197.
7. R. H. DAUSKARDT, M. R. JAMES, J. R. PORTER and R. O. RITCHIE, *J. Am. Ceram. Soc.* **75** (1992) 759.
8. K. WALKER, *ASTM STP 462* (American Society for Testing and Materials, Philadelphia, 1970) p. 1.
9. R. H. VAN STONE, *Mater. Sci. Eng.* **A103** (1988) 49.
10. R. O. RITCHIE and J. F. KNOTT, *Acta Metall.* **21** (1973) 639.
11. P. F. BECHER, *J. Am. Ceram. Soc.* **66** (1983) 485.
12. P. F. BECHER and M. K. FERBER, *Acta Metall.* **33** (1985) 1217.
13. P. F. BECHER, *J. Mater. Sci.* **21** (1986) 297.
14. P. F. BECHER, C. H. HSEUH, P. ANGELINI and T. N. TIEGS, *J. Am. Ceram. Soc.* **71** (1988) 1050.
15. P. F. BECHER, E. R. FULLER, Jr., and P. ANGELINI, *J. Am. Ceram. Soc.* **74** (1991) 2131.
16. ASTM Standard E647-88a, "Standard Test Method for Measurement of Fatigue Crack Growth Rates" in "1989 ASTM Annual Book of Standards", Vol. 3.01 (American Society for Testing and Materials, Philadelphia, 1989), p. 646.
17. R. H. DAUSKARDT and R. O. RITCHIE, *Closed Loop* **17** (1989) 7.
18. P. K. LIAW, H. R. HARTMANN and W. A. LODGSON, *J. Test. Eval.* **11** (1983) 202.

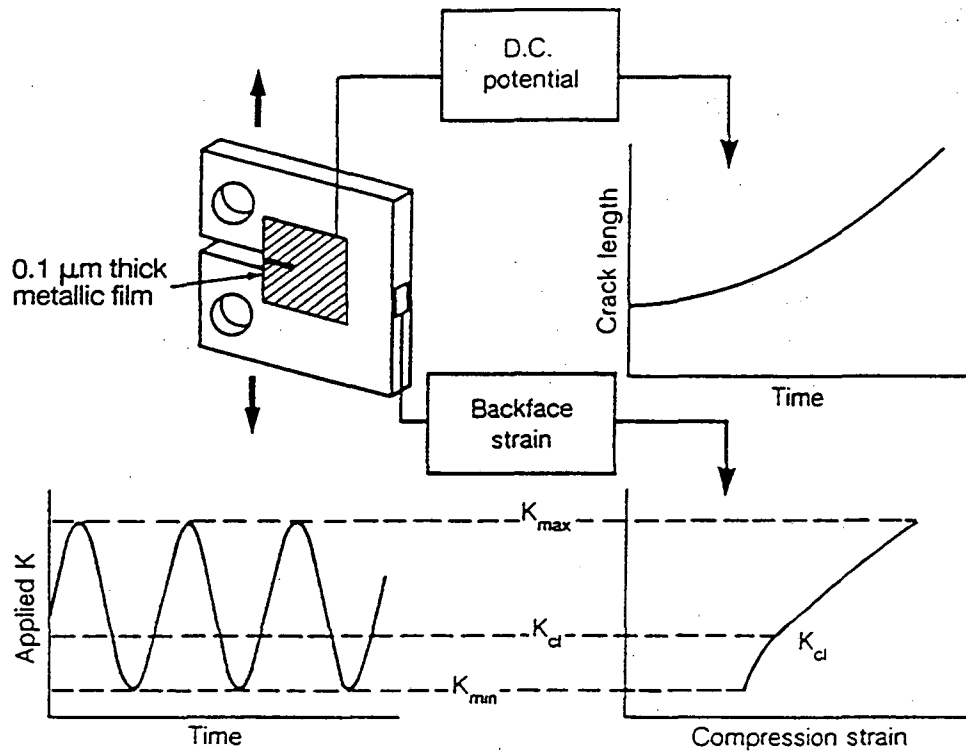
19. R. O. RITCHIE and W. YU, in "Small Fatigue Cracks", edited by R. O. Ritchie and J. Lankford (TMS-AIME, Warrendale, 1986), p. 167.
20. W. ELBER, in "Damage Tolerance in Aircraft Structures", ASTM STP 486 (American Society for Testing and Materials, Philadelphia, 1971), p. 230.
21. S. SURESH and R. O. RITCHIE, in "Fatigue Crack Growth Threshold Concepts", edited by D. L. Davidson and S. Suresh (TMS-AIME, Warrendale, 1984), p. 227.
22. C. M. WARD-CLOSE and R. O. RITCHIE, in "Mechanics of Fatigue Crack Closure", ASTM STP 982 (American Society for Testing and Materials, Philadelphia, 1988), p. 93.
23. R. H. DAUSKARDT, D. B. MARSHALL and R. O. RITCHIE, *J. Am. Ceram. Soc.* **73** (1990) 893.
24. A. G. EVANS, in "Fracture Mechanics: Perspectives and Directions (Twentieth Symp.)", ASTM STP 1020 (American Society for Testing and Materials, Philadelphia, 1989), p. 267.
25. R. COOK and B. R. LAWN, *J. Am. Ceram. Soc.* **66** (1983) C200.
26. R. O. RITCHIE, *Int. Met. Rev.* **20** (1979) 205.
27. P. F. BECHER, T. N. TIEGS, J. C. OGLE and W. A. WARWICK, in "Fracture Mechanics of Ceramics", Vol. 7, edited by R. C. Bradt, A. G. Evans, D. P. H. Hasselman and F. F. Lange (Plenum, New York, 1986), p. 61.
28. P. F. BECHER, *J. Am. Ceram. Soc.* **74** (1991) 255.
29. P. ANGELINI, W. MADER and P. F. BECHER, in "Advanced Structural Ceramics, MRS Proceedings", Vol. 78, edited by P. F. Becher, M. V. Swain and S. Somiya (Materials Research Society, Pittsburgh, 1987), p. 241.
30. J. J. PETROVIC and R. C. HOOVER, *J. Mater. Sci.* **22** (1987) 517.
31. J. RÖDEL, E. R. FULLER, Jr., and B. R. LAWN, *J. Am. Ceram. Soc.* **74** (1991) 3154.

32. P. L. SWANSON, C. J. FAIRBANKS, B. R. LAWN, Y. W. MAI and B. J. HOCKEY, *J. Am. Ceram. Soc.* **70** (1987) 279.
33. G. VEKINIS, M. F. ASHBY and P. W. R. BEAUMONT, *Acta Metall. Mater.* **38** (1990) 115.
34. S. LATHABAI, J. RÖDEL and B. R. LAWN, *J. Am. Ceram. Soc.* **74** (1991) 1340.
35. R. O. RITCHIE, R. H. DAUSKARDT, W. YU and A. M. BRENDZEL, *J. Biomed. Mater. Res.* **24** (1990) 189.
36. F. GUIU, M. J. REECE and D. A. J. VAUGHAN, *J. Mater. Sci.* **26** (1991) 3275.
37. H. KISHIMOTO, A. UENO and H. KAWAMOTO, in "Fatigue of Advanced Materials", edited by R. O. Ritchie, R. H. Dauskardt and B. N. Cox (Materials and Component Engineering Publications Ltd., Birmingham, UK, 1991) p. 255.
38. X.-Z. HU and Y.-W. MAI, *J. Am. Ceram. Soc.* **75** (1992) in press.



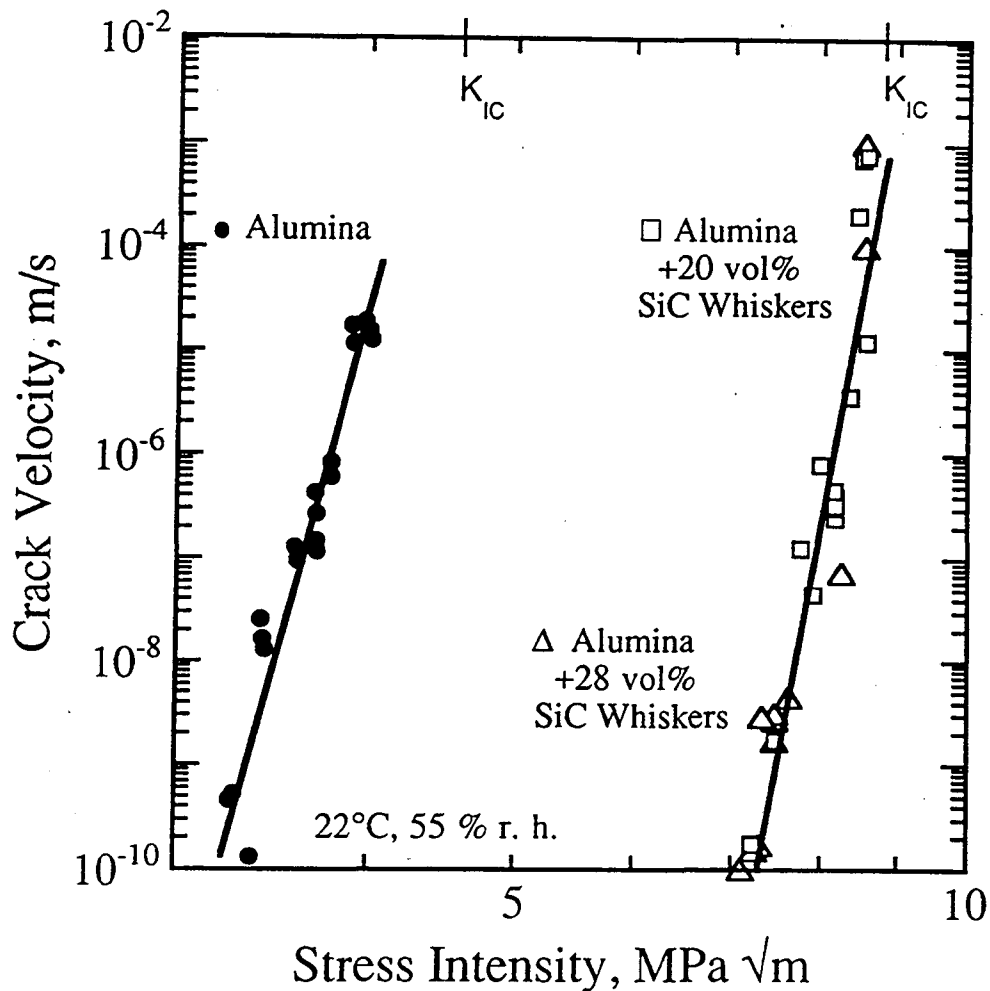
XBB 910-9112

Fig. 1. Scanning electron micrographs of a) the microstructure of the SiC-whisker reinforced alumina, showing b) local porosity centered at whisker clusters.



XBL 882-420D  
[Part (a)]

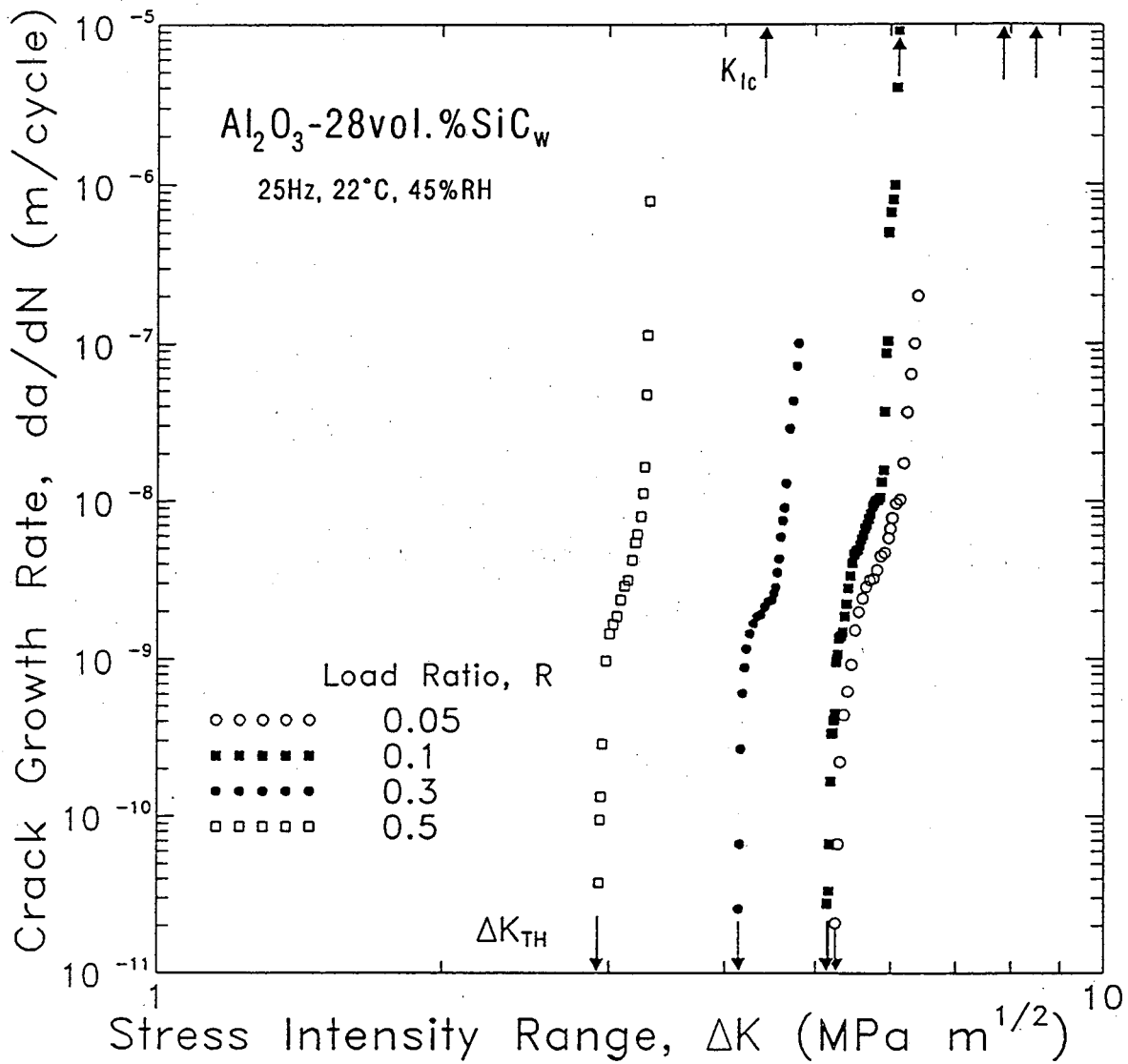
Fig. 2. Experimental techniques used to measure cyclic fatigue-crack growth rates, showing compact-tension C(T) specimen and procedures used to monitor crack length and the stress intensity  $K_{\text{cl}}$  at crack closure for "long" through-thickness cracks.



XBL 928-1913

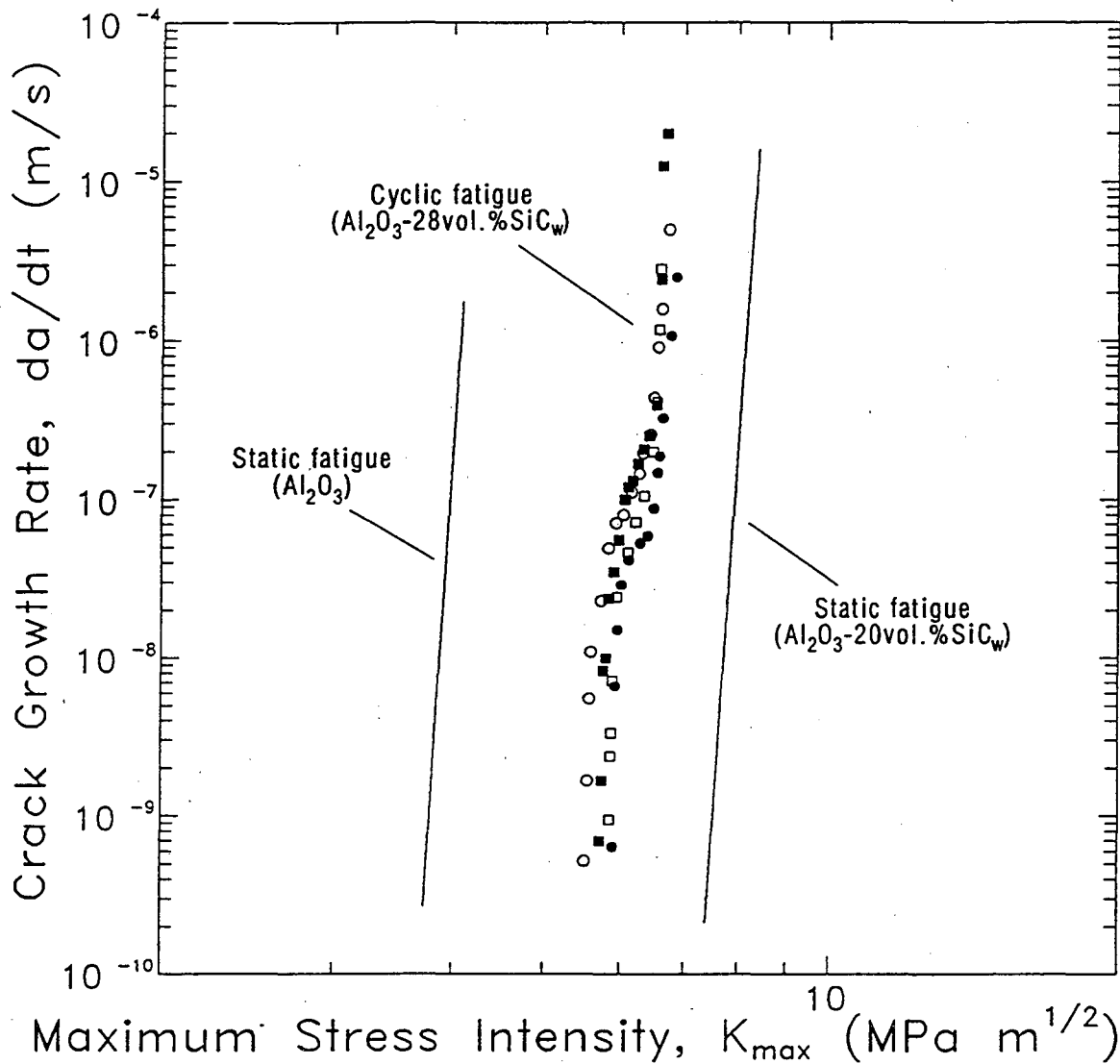
Fig. 3. The onset of static fatigue-crack growth for crack velocities  $\geq 10^{-10}$  m/s is initiated at higher applied stress intensities  $K$  in SiC whisker-reinforced aluminas as compared to a monolithic alumina ceramic. The rate of crack growth is very sensitive to changes in the applied stress intensity in each material. Composite data shown for  $\text{Al}_2\text{O}_3$ -20 vol.%  $\text{SiC}_w$  and  $\text{Al}_2\text{O}_3$ -28 vol.%  $\text{SiC}_w$ .





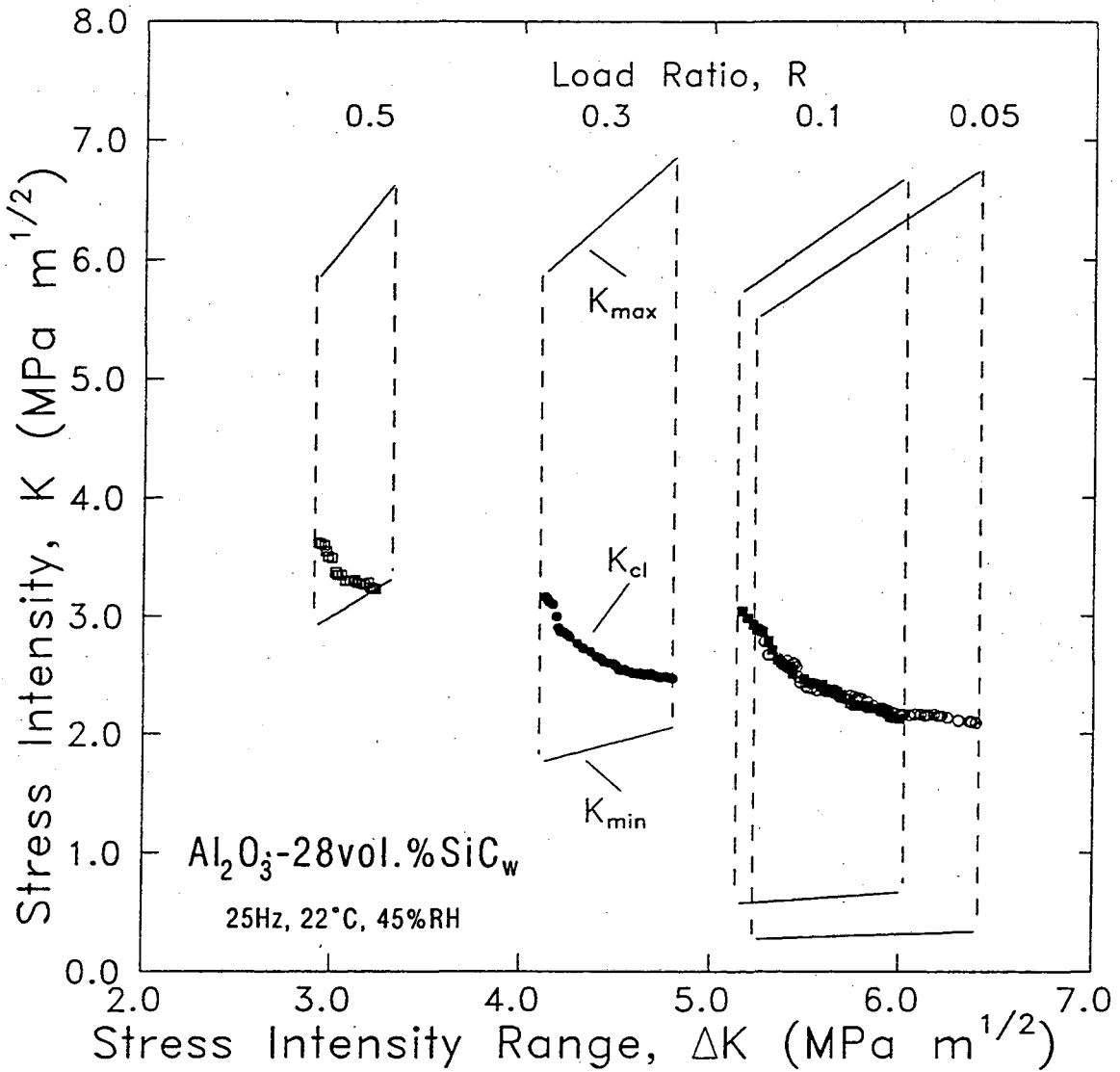
XBL 9111-2430

Fig. 4. Variation in cyclic fatigue-crack growth rates,  $da/dN$ , in  $\text{Al}_2\text{O}_3\text{-28 vol.\% SiC}_w$  ceramic composite with the applied stress-intensity range ( $\Delta K = K_{\max} - K_{\min}$ ), for load ratios of 0.05, 0.1, 0.3, and 0.5. Tests are performed at 25 Hz frequency in ambient temperature air.



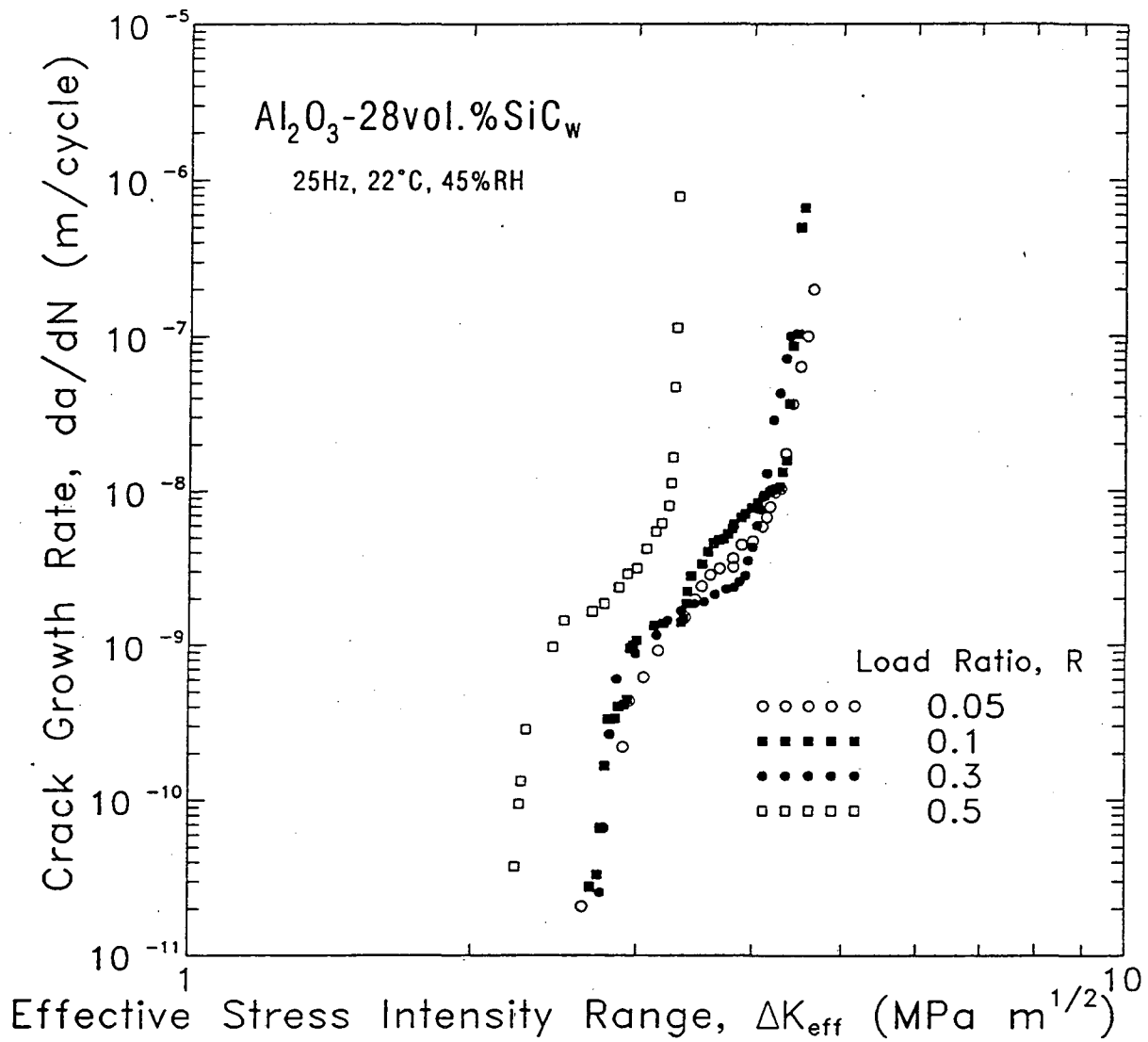
XBL 9111-2415

Fig. 5. Comparison of cyclic fatigue-crack velocities, as a function of time,  $da/dt$ , in  $Al_2O_3-28 vol. \% SiC_w$  ceramic composite in ambient temperature air with the applied maximum stress intensity  $K_{max}$  ( $R = 0.05 - 0.5$ ), with corresponding crack-velocity data for both unreinforced  $Al_2O_3$  and  $Al_2O_3-SiC_w$  obtained under monotonic loading (stress corrosion, static fatigue). Static fatigue data from Fig. 3.



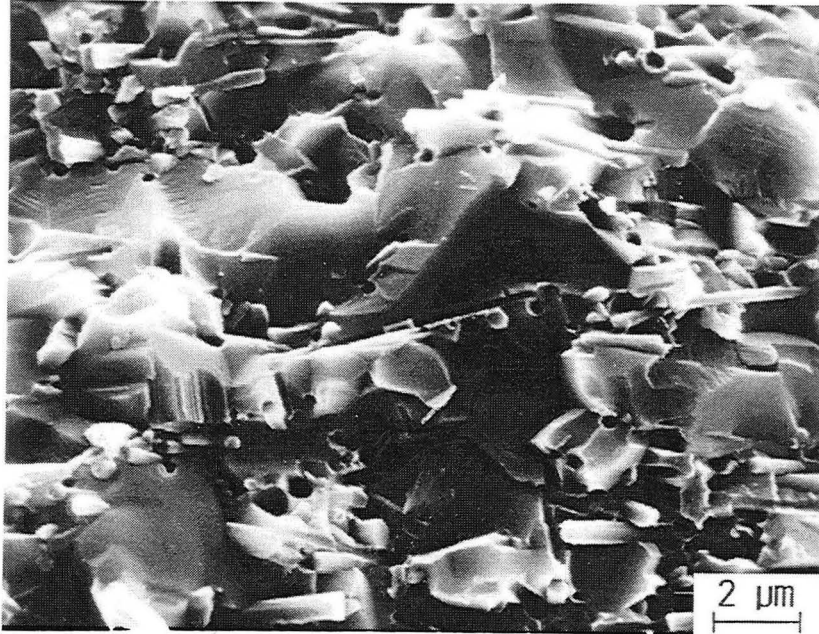
XBL 9111-2425

Fig. 6. Experimentally measured variation in the stress intensity at closure,  $K_{cl}$ , with the applied stress-intensity range,  $\Delta K$ , in  $Al_2O_3$ -28 vol.%  $SiC_w$  ceramic composite during cyclic fatigue in ambient temperature air for load ratios of 0.05, 0.1, 0.3, and 0.5. Applied values of  $K_{max}$  and  $K_{min}$  are shown for comparison.



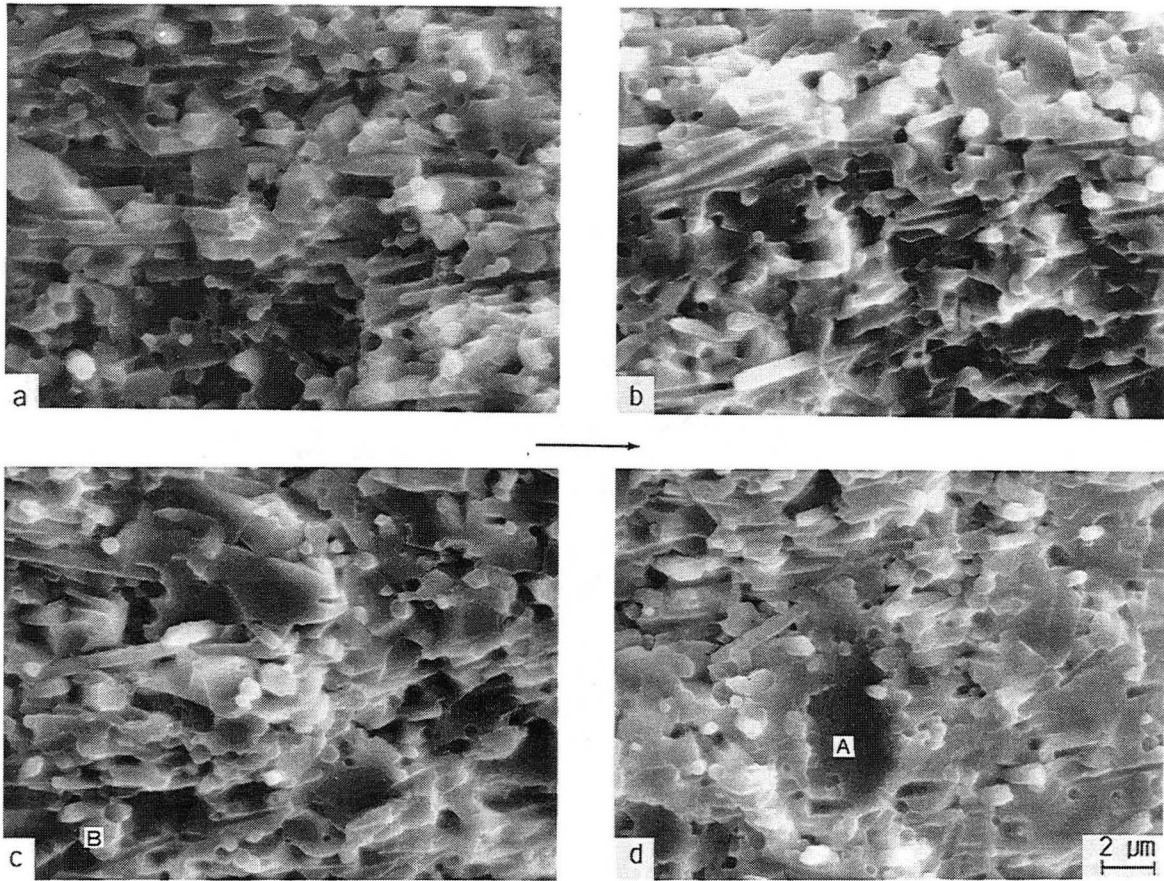
XBL 9111-2424

Fig. 7. Variation in cyclic fatigue-crack growth rates,  $da/dN$ , in  $\text{Al}_2\text{O}_3\text{-28 vol.\% SiC}_w$  ceramic composite at ambient temperature with the effective stress-intensity range ( $\Delta K_{\text{eff}} = K_{\text{max}} - K_{\text{cl}}$ ), for load ratios of 0.05, 0.1, 0.3, and 0.5.



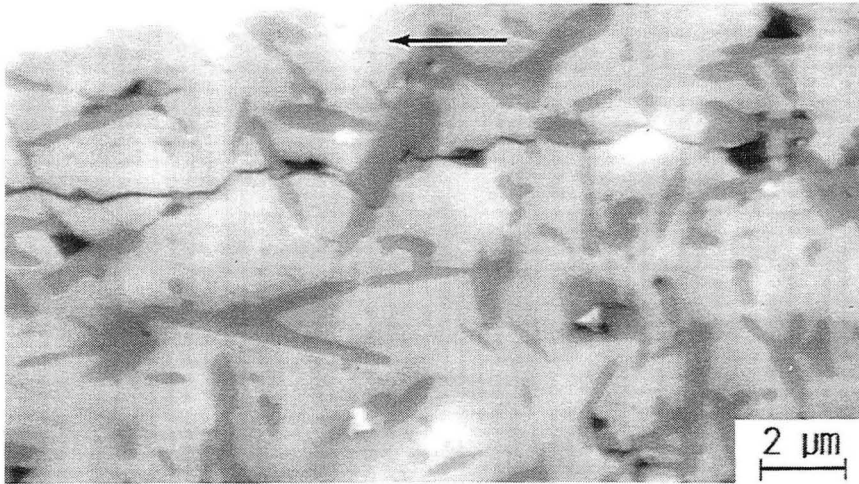
XBB 923-2119

Fig. 8. Extensive transgranular fracture of the alumina grains and pullout of the SiC whiskers are observed on fracture surfaces produced at high crack velocities in the larger grained alumina reinforced with 20 vol.% SiC whiskers, during static fatigue-crack growth.



XBB 921-368

Fig. 9. Scanning electron micrographs showing the fractography of cyclic fatigue-crack propagation in  $\text{Al}_2\text{O}_3$ -28 vol.%  $\text{SiC}_w$  ceramic composite at load ratios of a) 0.05, b) 0.3, and c) 0.5, and of d) overload fracture. Regions of transgranular cleavage of matrix grains and  $\text{SiC}$  whisker fracture/pull out are indicated by the letters *A* and *B*, respectively. Arrow indicates the general direction of crack growth.



XBB 921-369

Fig. 10. Scanning electron micrograph of the profile of a cyclic fatigue crack in  $\text{Al}_2\text{O}_3$ -28 vol.%  $\text{SiC}_w$  ceramic composite at a load ratio of 0.05. Note that the crack path follows regions of local porosity (marked by the letter *C*), and results in both whisker fracture (marked *D*) and failure along whisker/matrix interfaces (marked *E*) with little evidence of crack deflection, except at large  $\text{SiC}$  whiskers (marked *F*). Arrow indicates the general direction of crack growth.

LAWRENCE BERKELEY LABORATORY  
UNIVERSITY OF CALIFORNIA  
TECHNICAL INFORMATION DEPARTMENT  
BERKELEY, CALIFORNIA 94720